

Kinetics of the Reaction of CH₃S with O₃ at 298 KG. S. Tyndall[†] and A. R. Ravishankara*

National Oceanic and Atmospheric Administration, 325 Broadway, Boulder, Colorado 80303, and the Cooperative Institute for Research in Environmental Sciences, University of Colorado, Boulder, Colorado 80309 (Received: March 13, 1989)

Laser-induced fluorescence was used to detect CH₃S radicals in the laser flash photolysis of CH₃SH-O₃-H₂O-He (SF₆) mixtures. Evidence was found for a reaction between CH₃S and O₃, with a rate coefficient $(4.1 \pm 2.0) \times 10^{-12} \text{ cm}^3 \text{ molecule}^{-1} \text{ s}^{-1}$. The yield of CH₃S from the reaction OH + CH₃SH was determined to be 1.1 ± 0.2 . Our results suggest that the CH₃S + O₃ reaction could be the major sink for CH₃S in the atmosphere.

Introduction

Following measurements of large amounts of dimethyl sulfide (DMS) and its oxidation products (SO₂ and CH₃SO₃H) in the marine troposphere,¹ there have been increased efforts to study the mechanism of atmospheric oxidation of DMS. Indirect studies using stable end product determinations inferred that the oxidation proceeds through the CH₃S radical,²⁻⁴ but no mechanism has been proposed which fully accounts for the transformations leading to final products. Rate coefficients for the reactions of CH₃S with NO₂, O₂, and NO have recently been measured where CH₃S was produced by pulsed laser photolysis and detected by pulsed laser induced fluorescence (LIF).⁵⁻⁷ We investigated the kinetics and mechanisms of the first two of these reactions and estimated the lifetime of CH₃S due to these reactions in the marine troposphere to be 5-6 s for reaction with NO₂ and >0.07 s for reaction with O₂.⁶

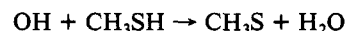
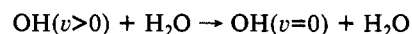
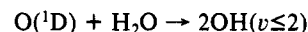
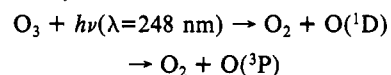
The reaction of CH₃S with O₃, the other major oxidant in the troposphere, had been discounted following a report that the reaction was relatively slow.⁷ In view of the reactivity of O₃ with other free radicals, particularly HS (which is analogous to CH₃S in reactivity toward NO₂ and O₂),⁸⁻¹⁰ and the relatively large abundance (tens of ppb; 1 ppb = a mole fraction of 10⁻⁹) of O₃ throughout the background troposphere, we decided to examine this reaction. We show here that the reaction between CH₃S and O₃ is in fact quite rapid and it could be the major sink for CH₃S in the atmosphere.

Experimental Section

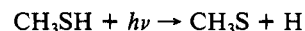
The experimental apparatus used in the present study is described in our previous paper on CH₃S reactions with NO₂ and O₂.⁶ In the present experiments CH₃S radicals were produced by pulsed 248-nm laser photolysis of CH₃SH-H₂O-O₃ mixtures in He or SF₆ and detected by pulsed LIF. The detection system was identical with that described previously except that an excimer-pumped dye laser was used in place of a Nd:YAG pumped dye laser with frequency mixing. The excimer-pumped dye laser directly produces 371.4 nm needed to excite the CH₃S ($\tilde{A}-\tilde{X}$) transition. Other workers have found complications attributed to heterogeneous reactions between O₃ and organic sulfides,^{10,11} so our system was modified to reduce the occurrence of heterogeneous reactions. The CH₃SH in He was added down a movable inlet at the top of the cell while the other gases were flowed in from one of the side arms. The gases were pumped out through the second side arm. This arrangement reduced the contact time of the CH₃SH with the O₃ prior to the reaction zone where CH₃S is created and detected. After exiting the cell all the effluent gases passed through a 50-cm cell equipped with a low-pressure Hg lamp and a photodiode detector to check the bulk composition of the mixture via absorption at 254 nm. It was found that a slight

decrease in O₃ absorbance occurred when CH₃SH was present, but this was shown to be due to chain reactions initiated by photolysis of the O₃ by the Hg lamp itself.

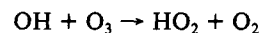
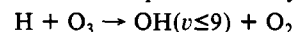
In our previous work on the reactions of CH₃S with NO₂ and O₂, CH₃S was produced by the laser photolysis of dimethyl disulfide (DMDS). However, it was found that a large loss of O₃ occurred in the presence of DMDS. Therefore, a new source of CH₃S was sought. Photolysis of O₃ at 248 nm was used to produce O(¹D) which reacted with H₂O. The OH in turn reacted with CH₃SH to give CH₃S. Use of He or SF₆ buffer gas allowed minimal quenching of O(¹D) to O(³P) before it reacted with H₂O. The H₂O also served to relax vibrationally excited OH which is formed from the reaction of O(¹D) with H₂O. The important reactions in this system are



A minor source of CH₃S is the direct photolysis of CH₃SH at 248 nm:



Other reactions that can take place in this system are



The products of the H + CH₃SH reaction are believed to be CH₃S + H₂ and CH₃ + H₂S.¹² The yield of CH₃S in the O + CH₃SH reaction is quite small.¹³ The complications that may

(1) Andreae, M. O.; Berresheim, H.; Andreae, T. W.; Kritiz, M. A.; Bates, T. S.; Merrill, J. T. *J. Atmos. Chem.* **1988**, *6*, 149.

(2) Niki, H.; Maker, P. D.; Savage, C. M.; Breitenbach, L. P. *Int. J. Chem. Kinet.* **1983**, *15*, 647.

(3) Hatakeyama, S.; Akimoto, H. *J. Phys. Chem.* **1983**, *87*, 2387.

(4) Grosjean, D. *Environ. Sci. Technol.* **1984**, *18*, 460.

(5) Balla, R. J.; Nelson, H. H.; McDonald, J. R. *Chem. Phys.* **1986**, *109*, 101.

(6) Tyndall, G. S.; Ravishankara, A. R. *J. Phys. Chem.* **1989**, *93*, 2426.

(7) Black, G.; Jusinski, L. E. *J. Chem. Soc., Faraday Trans. 2* **1986**, *82*, 2143.

(8) Friedl, R. R.; Brune, W. H.; Anderson, J. G. *J. Phys. Chem.* **1985**, *89*, 5505.

(9) Schönlé, G.; Rahman, M. M.; Schindler, R. N. *Ber. Bunsen-Ges. Phys. Chem.* **1987**, *91*, 66.

(10) Wang, N. S.; Howard, C. J. To be submitted for publication in *J. Phys. Chem.*

(11) Black, G. *J. Chem. Phys.* **1984**, *80*, 1103.

(12) Martin, D.; Jourdain, J. L.; LeBras, G. *Int. J. Chem. Kinet.* **1988**, *20*, 897, and references therein.

(13) (a) Cvetanovic, R. J.; Singleton, D. L.; Irwin, R. S. *J. Am. Chem. Soc.* **1981**, *103*, 3530. (b) Slagle, I. R.; Graham, R. E.; Gutman, D. *Int. J. Chem. Kinet.* **1976**, *8*, 451.

[†] Present address: National Center for Atmospheric Research, P.O. Box 3000, Boulder, CO 80307-3000.

* Correspondence should be addressed to this author at the National Oceanic and Atmospheric Administration, ERL, R/E/AL2, 325 Broadway, Boulder, CO 80303.

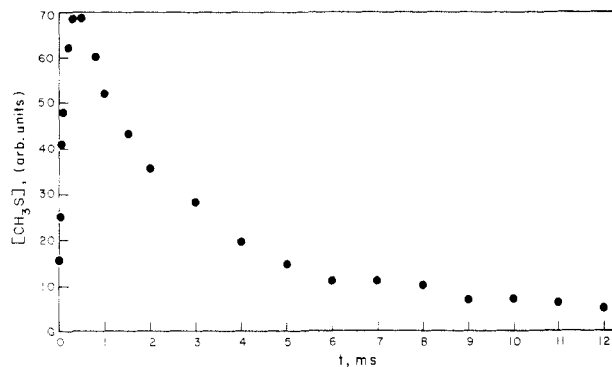


Figure 1. Temporal profile of $[\text{CH}_3\text{S}]$ in the presence of $7.9 \times 10^{13} \text{ cm}^{-3}$ of O_3 , $6.4 \times 10^{14} \text{ cm}^{-3}$ of CH_3SH , $1.2 \times 10^{16} \text{ cm}^{-3}$ of H_2O , and 150 Torr of He at 298 K. The growth in $[\text{CH}_3\text{S}]$ is due to the $\text{OH} + \text{CH}_3\text{SH}$ reaction. The maximum $[\text{CH}_3\text{S}]$ corresponds to $\sim 2 \times 10^{11} \text{ cm}^{-3}$. The nonexponential nature of CH_3S decay is evident from the signal not reaching zero at long reaction times.

arise from these reactions are that CH_3S is regenerated on the time scale of the experiment or that significant concentrations of O_3 are lost via chain reactions. However, by constraining the concentrations of H_2O , $(8\text{--}17) \times 10^{15}$ molecules cm^{-3} , and CH_3SH , $(2\text{--}10) \times 10^{14}$ molecules cm^{-3} , these complications were minimized.

The reaction between OH and CH_3SH has never been directly shown to give CH_3S as a product. It has been speculated that the reaction occurs by a complex addition mechanism.¹⁴ We could measure the yield of CH_3S in this reaction by using CH_3S produced from CH_3SH photolysis as an actinometer.

O_3 and CH_3SH were both used as dilute mixtures in He or, for a few experiments, in N_2 . The composition of the mixtures was frequently checked by diverting the mixture directly into the absorption cell. The absorption cross sections used at 254 nm were $1.16 \times 10^{-17} \text{ cm}^2 \text{ molecule}^{-1}$ for O_3 ¹⁵ and $2.1 \times 10^{-19} \text{ cm}^2 \text{ molecule}^{-1}$ for CH_3SH (spectrum from ref 16 normalized to the absorption cross section value at 248 nm from ref 17).

Results

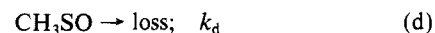
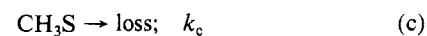
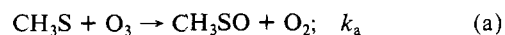
Photolysis of $\text{CH}_3\text{SH}\text{--O}_3\text{--H}_2\text{O}\text{--He}$ (SF_6) mixtures produces CH_3S . A typical temporal profile of CH_3S LIF signal is shown in Figure 1. Such temporal profiles were measured with O_3 concentrations in the range $(1\text{--}12.5) \times 10^{13}$ molecules cm^{-3} . At the lowest O_3 concentrations $[\text{CH}_3\text{S}]$ appeared to decay by first-order kinetics, but as the O_3 concentration increased, regeneration of CH_3S was observed. By tuning the excitation laser off the CH_3S absorption, it was ascertained that only CH_3S was being detected even in the time regime where the temporal profiles were nonexponential. Therefore, the nonexponential temporal profiles are due only to CH_3S regeneration. A nonlinear least-squares program was used to fit the decays to a biexponential function

$$[\text{CH}_3\text{S}] = A \exp(-k_f t) + B \exp(-k_s t) \quad (\text{I})$$

where k_f represents the initial (fast) decay of CH_3S and k_s the long-time (slow) decay. A plot of k_f vs $[\text{O}_3]$ was linear, and it is proposed that this primarily represents the removal of CH_3S by reaction with O_3 . The slow decay constant, k_s , showed no systematic dependence on $[\text{O}_3]$, and probably represents diffusion out of the detection zone in our system.

The general kinetic behavior we observed in this system is typical of a mechanism where the product C of reaction $\text{A} + \text{B}$ reacts with reactant A to generate B, the species whose temporal profile is being monitored. In this case the following mechanism

would explain the observations that were made:



Note that reaction b may not be an elementary reaction but is the rate-limiting step in the regeneration of CH_3S in our system and that reactions c and d include reactions of CH_3S and CH_3SO with O_3 that do not produce CH_3SO and CH_3S , respectively. This reaction mechanism can be solved to obtain the following equation for the temporal profile of CH_3S :

$$[\text{CH}_3\text{S}] = [\text{CH}_3\text{S}]_0 (C_1 - C_2)^{-1} \{ (d + C_1) \exp(C_1 t) - (d + C_2) \exp(C_2 t) \} \quad (\text{II})$$

where

$$C_1 = 0.5\{(a^2 - 4b)^{0.5} - a\}$$

$$C_2 = -0.5\{(a^2 - 4b)^{0.5} + a\}$$

$$d = k_b[\text{O}_3] + k_d$$

$$a = k_a[\text{O}_3] + k_b[\text{O}_3] + k_c + k_d$$

$$b = k_a k_d [\text{O}_3] + k_b k_c [\text{O}_3] + k_c k_d$$

Unfortunately, we cannot easily use this equation to obtain k_a , k_b , k_c , and k_d since (i) temporal profiles of required quality to fit such an expression were unobtainable, (ii) k_a and k_b are not substantially different from one another, (iii) the initial CH_3S generation step must be included, and (iv) the experimental parameters could not be varied over wide enough ranges to make these fits meaningful. However, we could simplify expression II because of the following observations: when CH_3S profiles were measured in the presence of $\sim 3 \times 10^{14} \text{ cm}^{-3}$ of O_3 , CH_3S concentrations rapidly reached values ~ 0.2 times the initial values after which time they decayed with a pseudo-first-order rate coefficient of $\sim 50 \text{ s}^{-1}$. The loss rate of CH_3S in the absence of O_3 was also $\sim 50 \text{ s}^{-1}$. The simplifications that can be made from the above observations are (i) $k_c \approx k_d$ and (ii) there is very little loss of CH_3S and CH_3SO due to reactions with O_3 that do not produce CH_3SO and CH_3S , respectively. Under these conditions, it can be shown that eq II reduces to eq I, which was used to fit the data, where

$$k_f = k_a[\text{O}_3] + k_b[\text{O}_3] + k_c \text{ (or } k_d)$$

and

$$k_s \approx k_c$$

The first-order loss rate for CH_3S was estimated from experiments conducted in the absence of O_3 . Since the quality of the fits to eq I was strongly influenced by the number of data points in the temporal profile taken at longer time, k_c was usually fixed at the value found in the absence of O_3 or at the values derived from fits to experiments with high O_3 . The value of k_c chosen ranged from 50 to 65 s^{-1} . Less than 10% variation in the fitted value k_f was found when k_c was changed to either 45 or 75 s^{-1} , the extreme values likely for this rate coefficient.

According to the above analysis, a plot of k_f against $[\text{O}_3]$ should be linear, with a slope of $(k_a + k_b)$ and an intercept of k_c . A plot of $k_f - k_c (= k_a' + k_b' = k_a[\text{O}_3] + k_b[\text{O}_3])$ is shown in Figure 2. The estimated errors on individual points are $\pm(10\text{--}15)\%$, due to the uncertainties generated in fitting a biexponential form to the data where two reaction rate coefficients are of similar magnitude. Nevertheless, the expected dependence on O_3 concentration is found. A linear unweighted regression line through the data points gives

$$(k_a + k_b) = (5.1 \pm 0.6) \times 10^{-12} \text{ cm}^3 \text{ molecule}^{-1} \text{ s}^{-1}$$

where the error bar is 2σ and refers to precision only.

(14) Hynes, A. J.; Wine, P. H. *J. Phys. Chem.* **1987**, *91*, 3672.

(15) Molina, L. T.; Molina, M. J. *J. Geophys. Res.* **1986**, *91*, 14501.

(16) Calvert, J. G.; Pitts, J. N., Jr. *Photochemistry*; Wiley: New York, 1966.

(17) Wine, P. H.; Nicovich, J. M.; Hynes, A. J.; Wells, J. R. *J. Phys. Chem.* **1986**, *90*, 4033.

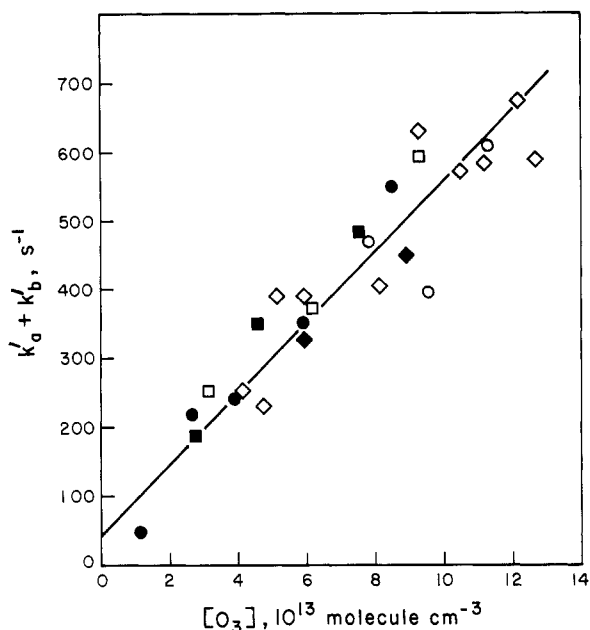


Figure 2. Plot of $k_f - k_c (= k'_a + k'_b = k_a[O_3] + k_b[O_3])$, the first-order loss rate of CH_3S to the stationary state, as a function of $[O_3]$. Symbols: ■, 50 Torr of He; □, 100 Torr of He; ○, 150 Torr of He; ●, 200 Torr of He; ◆, 70 Torr of SF_6 ; ◇, 100 Torr of SF_6 .

An estimate of the relative magnitudes of k_a and k_b can be obtained from the magnitudes of A and B in eq I. The initial CH_3S concentration is proportional to $(A + B)$ whereas B represents the "stationary-state" concentration of CH_3S extrapolated back to the photolysis laser pulse. Thus

$$\frac{[CH_3SO]_e}{[CH_3S]_e} = \frac{k_a}{k_b} = \frac{A}{B} \quad (III)$$

or

$$\frac{k_a}{k_a + k_b} = \frac{A}{A + B} \quad (IV)$$

where $[CH_3SO]_e$ and $[CH_3S]_e$ represent the concentrations in the "stationary state". The expression IV was used, since the sum $A + B$ was found to be very insensitive to the fitted values of k_f and k_c , whereas the value of B returned could vary by up to 50%.

For the experiments carried out in SF_6 the ratio $k_a/(k_a + k_b)$ was found to be (0.75 ± 0.1) , while in He a ratio (0.85 ± 0.1) was found. The error bars are 2σ . Taking $k_a/(k_a + k_b) = 0.8$ and $(k_a + k_b) = 5.1 \times 10^{-12} \text{ cm}^3 \text{ molecule}^{-1} \text{ s}^{-1}$ yields $k_a = 4.1 \times 10^{-12} \text{ cm}^3 \text{ molecule}^{-1} \text{ s}^{-1}$.

The maximum CH_3S concentration was also found to increase linearly with the O_3 concentration, indicating that $OH + CH_3SH$ does indeed give CH_3S . The total concentration of CH_3S produced is given by

$$[CH_3S] \approx 2F(\sigma_c[CH_3SH] + 0.9\sigma_o[O_3]\Phi_r)$$

where

F = laser fluence

σ_c = CH_3SH cross section at 248 nm

σ_o = O_3 cross section at 248 nm

Φ_r = yield of CH_3S from $OH + CH_3SH$

and the factor 0.9 takes account of the $O(^1D)$ quantum yield from O_3 photolysis. It is assumed that every $O(^1D)$ reacts with H_2O .

A plot of the CH_3S concentration, normalized to the photolysis laser fluence, versus $[O_3]$ is shown in Figure 3 for one series of experiments where the CH_3SH concentration was held constant. The intercept is equal to twice the yield of CH_3S found in an experiment with no O_3 present. The slope is proportional to Φ_r . To avoid having to measure F , we can use the ratio of the slope

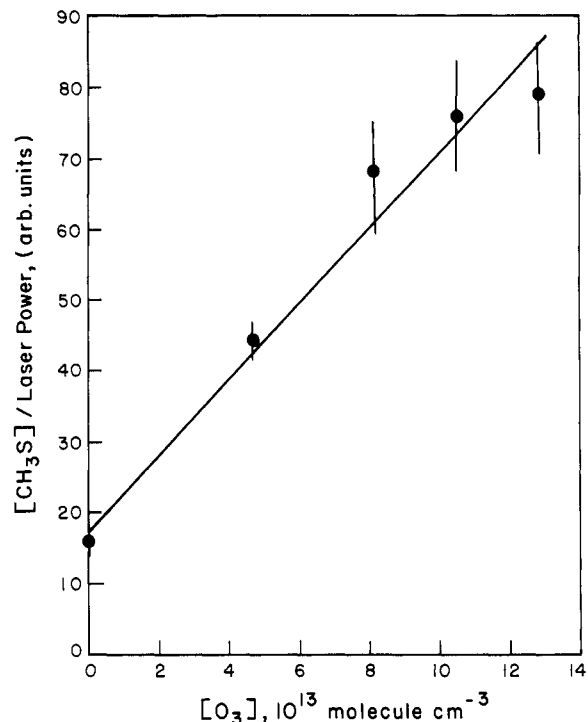
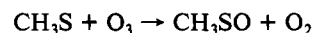


Figure 3. Plot of CH_3S yield normalized to a constant laser fluence versus $[O_3]$. $[CH_3SH] = 1.05 \times 10^{15} \text{ cm}^{-3}$, total pressure 96 Torr of SF_6 , and laser fluence $\approx 1 \times 10^{14} \text{ photons cm}^{-2}$.

to intercept, $(0.9\sigma_o\Phi_r/2\sigma_c[CH_3SH])$, from which Φ_r is calculated. The results of three such series of experiments with different concentrations of CH_3SH and laser fluence yield $\Phi_r = 1.1 \pm 0.2$. The quoted error is 2σ and includes estimated systematic errors. This is the first direct measurement of the product yield in the reaction of OH with an organic sulfide.

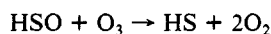
Discussion

The work described here suggests that CH_3S reacts rapidly with O_3 , presumably to form $CH_3SO + O_2$.



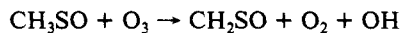
This reaction is analogous to the reaction of HS with O_3 to give HSO . The only previous attempt to study this reaction was by Black and Jusinski,⁷ who used much larger concentrations of both O_3 and CH_3S . They found no evidence for a reaction and estimated $k \leq 8 \times 10^{-14} \text{ cm}^3 \text{ molecule}^{-1} \text{ s}^{-1}$. However, under their conditions ($[O_3] = 1.1 \times 10^{16} \text{ molecules cm}^{-3}$ and $[CH_3SH] = 7.7 \times 10^{14} \text{ molecules cm}^{-3}$) regeneration of CH_3S would have been so rapid that they would not have observed the initial decay. The exact mechanism for the CH_3S regeneration, i.e., reaction b, being an elementary step or proceeding via the formation of OH would not have mattered in their experiment. Also, H atoms produced in their system would have regenerated CH_3S on the time scale of the measurements via the sequence, $H + O_3 \rightarrow OH + O_2$ and $OH + CH_3SH \rightarrow CH_3S + H_2O$. By utilizing much lower concentrations of CH_3S ($\leq 10^{12} \text{ molecules cm}^{-3}$) and O_3 ($< 1.25 \times 10^{14} \text{ molecules cm}^{-3}$), we have avoided problems due to secondary chemistry and we are able to observe the actual decay of CH_3S radicals. Nevertheless, we must stress that the regeneration of CH_3S introduces uncertainty into our analysis. We feel reasonably confident that the range $k = (4.1 \pm 2.0) \times 10^{-12} \text{ cm}^3 \text{ molecule}^{-1} \text{ s}^{-1}$ encompasses uncertainties inherent in the analysis and the possible occurrence of a heterogeneous reaction between CH_3SH and O_3 . This value did not depend on the concentrations of CH_3SH and H_2O , laser fluence, pressure of the diluent gas, and the nature of the diluent gas, i.e., He or SF_6 . (see Figure 2). The intercept in Figure 2 is due to errors in our analyses and/or k_d being not equal to k_c . When the line is forced to go through the origin, the value $k_a + k_b$ we get is no more than 20% different from the quoted value.

The mechanism of the regeneration is not elucidated at this stage. Friedl et al.⁸ and Wang and Howard¹⁰ postulated that HSO reacts with O₃ to generate HS.



However, the analogous reaction for CH₃S would be endothermic by as much as 14 kcal mol⁻¹, based on Δ*H*_f^o for CH₃SO of -16 kcal mol⁻¹.¹⁸ It seems unlikely that the S-O bond energies in HSO and CH₃SO should differ by 14 kcal mol⁻¹. It should be noted that the thermochemistry of oxygenated sulfur-containing radicals is presently not very well defined.

A second explanation for the regeneration is production of OH radicals. A direct exothermic channel would be



for which Δ*H*^o = -20 kcal mol⁻¹. The above multistep mechanism cannot be excluded at this stage.

The impact of this reaction on the chemistry of the marine troposphere can not be determined directly. If the reaction results

in removal of CH₃S, then it will almost certainly be the dominant loss process for CH₃S. Using rate coefficients determined in this laboratory for the reactions of CH₃S with O₃, NO₂, and O₂, and typical tropospheric mixing ratios of 3 × 10⁻⁸, 1 × 10⁻¹⁰, and 0.21 for these compounds, we estimate first-order loss rates for CH₃S of 3.5 s⁻¹, 0.15 s⁻¹, and <13 s⁻¹, respectively. As discussed in our earlier paper, the rate coefficient for the O₂ reaction is possibly an order of magnitude lower than this upper limit. The fate of the reduced sulfur then depends on the reactions of CH₃SO. If CH₃SO reacts only with O₃ in the atmosphere to simply regenerate CH₃S, then the reactions will not constitute a loss for CH₃S or CH₃SO. However, if other molecules oxidize CH₃SO or the CH₃SO + O₃ reaction does not yield CH₃S, the conversion of CH₃S to CH₃SO will give the true lifetime of CH₃S. For example, if O₂ reacts with CH₃SO with a rate coefficient ≥ 2 × 10⁻¹⁹ cm³ molecule⁻¹ s⁻¹, then CH₃SO would be lost exclusively via this reaction in the atmosphere. Experimental studies on the kinetics and mechanisms of CH₃SO reactions are needed to understand the atmospheric oxidation pathway for CH₃S.

Acknowledgment. This work was supported by NOAA as a part of the National Acid Precipitation Assessment Program.

(18) Benson, S. W. *Chem. Rev.* 1978, 78, 23.

ARTICLES

Hydrogen Bonding and Reaction Specificity in Lactate Dehydrogenase Studied by Raman Spectroscopy

Hua Deng,[†] Jie Zheng,[†] John Burgner,^{*,‡} and Robert Callender^{*,†}

Physics Department, City College of the City University of New York, New York, New York 10031, and Department of Biological Sciences, Purdue University, West Lafayette, Indiana 47907

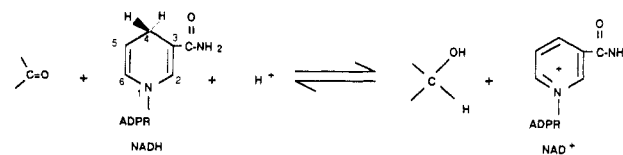
(Received: September 26, 1988; In Final Form: December 27, 1988)

The Raman spectrum of a small molecule or molecular moiety when bound to sizable proteins can be measured by using difference techniques developed in our laboratory. We have applied this method in obtaining the Raman spectrum of the cofactor acetylpyridine adenine dinucleotide, APAD⁺, when bound to lactate dehydrogenase. The Raman data permit a characterization of some of the molecular interactions responsible for the stereochemistry of the reaction catalyzed by this enzyme. We find that the enzyme forms a strong hydrogen bond with the cofactor's carboxamide group and suggest that this is at least partially responsible for the very high degree of stereochemistry fidelity observed with this enzyme.

Introduction

An important issue of enzymatic catalysis is that enzymes use noncovalent interactions to facilitate the making and breaking of covalent bonds and to perform stereospecific reactions.¹ The energy and origin of these noncovalent interactions are generally difficult to assess experimentally. In this paper, we investigate the origins of the bonds between enzyme and coenzyme that are at least partially responsible for the stereochemistry of the reaction catalyzed by lactate dehydrogenase and that are found generally in the pyridine-dependent dehydrogenases, using classical Raman spectroscopy. Raman spectroscopy provides detailed information concerning these molecular properties and the interactions between molecules and molecular groups.² For the study of small molecules at the active sites of proteins, much use has been made of resonance-enhanced Raman spectroscopy. The enhanced spectrum

SCHEME I



of the colored prosthetic group so dominates the protein classical Raman spectrum that it is easily detected despite its small relative mass. Unfortunately, this approach is limited to those cases where

(1) Reviewed in: (a) You, K. *Methods Enzymol.* 1982, 87, 101. (b) You, K. *CRC Crit. Rev. Biochem.* 1985, 17, 313. (c) Fersht, A. *Enzyme, Structure, and Mechanism*, 2nd ed.; Freeman: New York, 1985.

(2) Reviewed in: (a) *Biological Applications of Raman Spectroscopy*; Spiro, T., Ed.; Wiley: New York, 1987; Vols. I and II. (b) Carey, P. R. *Biochemical Applications of Raman and Resonance Raman Spectroscopy*; Academic Press: New York, 1982.

[†]City University of New York.

[‡]Purdue University.